Reliability-based design optimization by using support vector machines

Niclas Strömberg
Department of Mechanical Engineering
Örebro University, Sweden

ABSTRACT: In this work we perform reliability-based design optimization (RBDO) by classifying the limit states by using soft non-linear support vector machines (SVM). By adopting the kernel trick in the dual formulation, by using e.g. the Gaussian kernel, we classify non-linear states of fail or safe obtained from design of experiments. The most probable point (MPP) of the SVM is established in the physical space where the distance is minimized in the metric of Hasofer-Lind. The solution to the corresponding optimality conditions is obtained by using Newton's method with an inexact Jacobian and a line-search of Armijo type. At the MPP, we perform Taylor expansions of the SVM using intermediate variables defined by the iso-probabilistic transformation. In such manner, we derive a quadratic programming (QP) problem which is solved in the standard normal space. This is done for several probability distributions such as e.g. lognormal, Gumbel, gamma and Weibull. The optimal solution to the QP problem is mapped back to the physical space and new Taylor expansions of the SVM are derived and a new QP problem is formulated and solved. This procedure continues in sequence until we obtain convergence of our RBDO problem. The steps presented above constitute our proposed FORM-based sequential QP approach for RBDO by using SVM. The target of reliability appearing in the FORM-based QP problem might also be adjusted using different SORM formulas such as e.g. Breitung, Hohenbichler or Tvedt, or by applying importance-based Halton or Hammersley sampling. A nice feature of the proposed SVM-based RBDO approach is that several limit state functions can be represented simultaneously by only one single SVM. Thus, the proposed SVM-based RBDO methodology might be considered to be a rational approach for the treatment of RBDO problems including system reliability. This is demonstrated by solving established RBDO benchmarks.

1 INTRODUCTION

The soft non-linear support vector machine (SVM) introduced by Cortes & Vapnik (1995) defines a paradigm shift in machine learning and the paper has been cited more than 15000 times. By adopting the kernel trick and the soft penalization, we are able to classify non-linear separable data including misclassified data points. In this work, we suggest to use a single SVM to represent several limit state functions simultaneously when performing reliability based design optimization. For readers not familiar with SVM, an excellent introduction to this machine learning discipline is found in the textbook by Hamel (2009).

Although the number of papers on SVM-based RBDO is small, the idea of using SVM in order to represent limit state functions in RBDO is not new. Basudhar et al. (2008) solved RBDO problems using SVM and a particle swarm algorithm. Song et al. (2012) performed sampling-based RBDO by using probabilistic sensitivity analysis and virtual support vector machines. Khatibinia et al. (2013) suggested a gravitational search algorithm with a weighted least square support vector machine for RBDO. Wang et al. (2015) proposed a new SORA-based RBDO method using SVM as a surrogate model for the limit state function. Most recently Liu et al. (2017) used SVM-based sampling in order to improve Kriging models for RBDO. Another recent paper is by Yang & Husada (2017), who study seven state of the art methods from data mining in order to improve accuracy and efficiency of a single-loop RBDO method.

In this work, we will adopt the SORM-based sequential quadratic programming (SQP) approach for RBDO recently suggested by Strömberg (2017), where we now represent the limit state functions by using SVM instead of analytical expressions. The main idea of the proposed method is to represent several limit state functions simultaneously with only one single SVM. In such manner, a RBDO problem with several reliability constraints boil down to a problem with only one constraint. We also think that this approach is a step towards a rational method for treating problems with system reliability. Reliability analysis without optimization using a similar idea was recently investigated by Li et al. (2016).

The proposed method might be consider to be a metamodel-based approach for RBDO even though the SVM is not representing the overall behaviour of the reliability constraint function but only is a representation of the limit state or a classification of states in fail or safe. Metamodel-based RBDO is a most powerful approach for treating the reliability constraints of complex models such as non-linear finite element models. Popular metamodels for this kind of applications are e.g. Kriging (Hu et al. 2016), artificial neural networks (Zhu et al. 2011) and radial basis function networks (Lv et al. 2015). In Strömberg (2016) FORM- and SORM-based RBDO of a underrun protection profile was performed using a new type of radial basis function networks with a priori bias suggested by Amouzgar & Strömberg (2017).

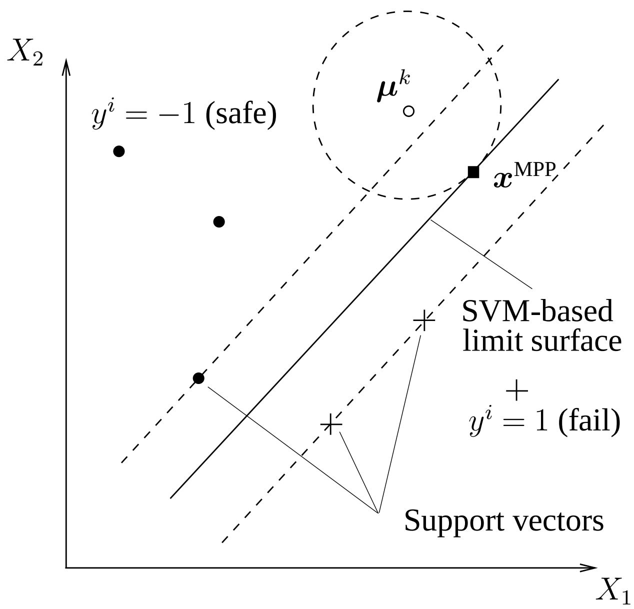

Figure 1: Illustration of the proposed SVM-based RBDO approach.

The outline of the paper is as follow: in the next section we review the FORM- and SORM-based SQP approach for reliability based design optimization that recently was suggested in Strömberg (2017), in section 3 we present the theory of the soft non-linear support vector machine by deriving the dual formulation of the maximum margin problem using the Karush-Kuhn-Tucker (KKT) conditions and introducing the soft penalization. In section 4 two RBDO examples are solved using the proposed SVM-based methodology, in particular an established benchmark with three reliability constraints are treated using a single SVM and we also suggest how to apply SVM-based adaptive sampling in order to improve the solution. Finally, some concluding remarks are presented.

2 SQP-BASED RBDO

Most recently a SORM-based SQP approach for RBDO was suggested in Strömberg (2017). A brief presentation of this approach is given in this section.

Let us consider the following RBDO problem:

$$\begin{cases} \min\limits_{\boldsymbol{\mu}} & f(\boldsymbol{\mu}) \\ \text{s.t.} & \Pr[g(\boldsymbol{X}) \leq 0] \geq P_s, \end{cases} \tag{1}$$

where $\boldsymbol{X}$ is a vector of N_{VAR} uncorrelated random variables X_i. The mean value μ_i of each variable X_i is collected in $\boldsymbol{\mu}$. The functions $f = f(\boldsymbol{\mu})$ and $g = (\boldsymbol{X})$ represent the objective function and constraint, respectively. Thus, the reliability constraint reads that the probability that $g \leq 0$ must be greater than the target of reliability P_s. In this work, we treat this reliability constraint by representing the limit state $g = 0$ by support vector machines, see the next section. The SVM can also be used to classify states of fail or safe, but that is not the main purpose of using SVM in this work. The main idea is to represent several limit states simultaneously by using a single SVM and then to perform RBDO following the method presented in this section.

The cumulative distribution of each variable is given by

$$F_i(x; \boldsymbol{\theta}_i) = \int_{-\infty}^{x} \rho_i \, \mathrm{d}x, \tag{2}$$

where $\rho_i = \rho_i(x; \boldsymbol{\theta}_i)$ is the probability density function for distributions parameters collected in $\boldsymbol{\theta}_i = \boldsymbol{\theta}_i(\mu_i)$. So far, the following distributions have been implemented: normal, lognormal, Gumbel, gamma and Weibull.

The problem in (1) is solved by the SQP approach as outlined below. At an iterate k with mean values collected in $\boldsymbol{\mu}^k$, we perform Taylor expansions of f and g in intermediate variables Y_i defined by the isoprobabilistic transformation, i.e.

$$Y_i = Y_i(X_i) = \Phi^{-1}\left(F_i(X_i; \boldsymbol{\theta}_i(\mu_i^k))\right), \tag{3}$$

where Φ=$\Phi(x)$ is the cumulative distribution of the standard normal distribution. In addition, the Taylor expansion of g is done at the most probable point x_i^{MPP} on the limit surface. The Taylor expansion of f becomes $f(\boldsymbol{\eta}) \approx f(\boldsymbol{\mu}^k)+$

$$\sum_{i=1}^{N_{\text{VAR}}} \frac{\partial f}{\partial X_i}\bigg|_{\boldsymbol{X}=\boldsymbol{\mu}^k} \frac{\phi(Y_i^k)}{\rho_i(\mu_i^k; \boldsymbol{\theta}_i^k)} \eta_i + \frac{1}{2} \sum_{i=1}^{N_{\text{VAR}}} \sum_{j=1}^{N_{\text{VAR}}} \tilde{H}_{ij} \eta_i \eta_j, \tag{4}$$

where $\boldsymbol{\eta}$ is the mean of $\boldsymbol{Y}$ and

$$\tilde{H}_{ij} = \frac{\partial^2 f}{\partial X_i \partial X_j}\bigg|_{\boldsymbol{X}=\boldsymbol{\mu}^k} \frac{\phi(Y_i^k)}{\rho_i(\mu_i^k; \boldsymbol{\theta}_i^k)} \frac{\phi(Y_j^k)}{\rho_j(\mu_j^k; \boldsymbol{\theta}_j^k)}. \tag{5}$$

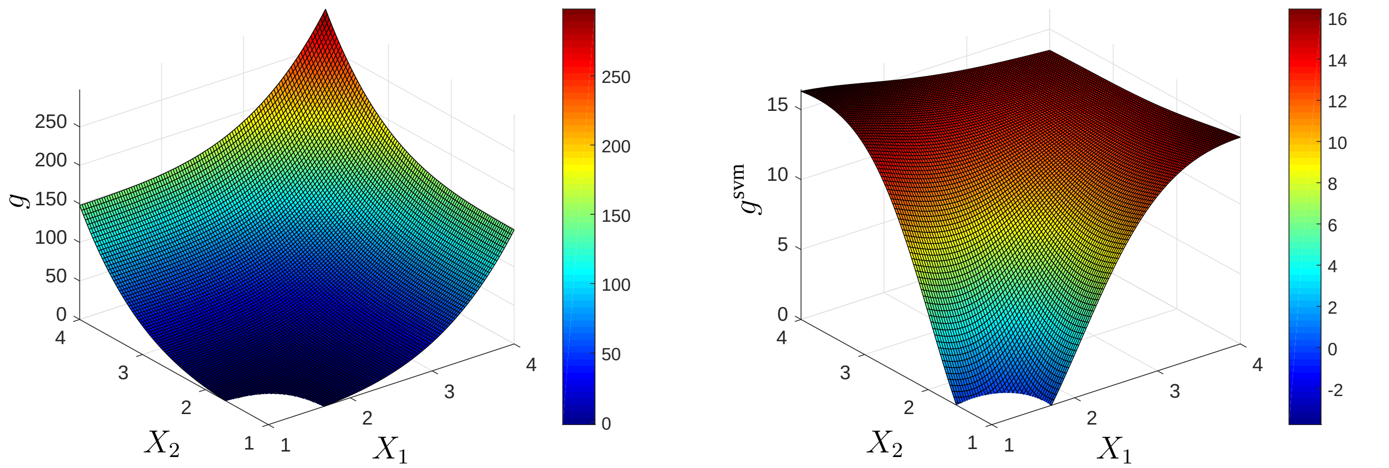

Figure 2: The left plot shows $g > 0$ and in the right plot $g^{\text{svm}} > 0$ is given. Despite the overall behaviour is not captured by the SVM, the limit state is represented properly.

Furthrmore, $\tilde{g} = \tilde{g}(\boldsymbol{Y}) \approx$

$$\sum_{i=1}^{N_{\text{VAR}}} \frac{\partial g}{\partial X_i}\bigg|_{\boldsymbol{X}=\boldsymbol{x}^{\text{MPP}}} \frac{\phi(y_i^{\text{MPP}})}{\rho_i(x_i^{\text{MPP}};\boldsymbol{\theta}_i^k)}\left(Y_i - y_i^{\text{MPP}}\right), \tag{6}$$

where $y_i^{\text{MPP}} = Y_i(x_i^{\text{MPP}})$ is the most probable point defined by

$$\begin{cases} \min\limits_{\boldsymbol{X}} \dfrac{1}{2}\boldsymbol{Y}(\boldsymbol{X})^T\boldsymbol{Y}(\boldsymbol{X}) \\ \text{s.t. } g(\boldsymbol{X}) = 0. \end{cases} \tag{7}$$

In this work, we solve (7) when the limit state $g(\boldsymbol{X}) = 0$ is represented by a soft non-linear SVM as presented in the next section. This is in turn done by solving the necessary optimality conditions by using Newton's method with an inexact Jacobian.

Finally, by inserting (4) and (6) into (1), we derive the following QP-problem:

$$\begin{cases} \min\limits_{\eta_i} & f(\boldsymbol{\eta}) \\ \text{s.t.} & \begin{cases} \mu_{\tilde{g}} \leq -\beta_t\sigma_{\tilde{g}}, \\ -\epsilon \leq \eta_i \leq \epsilon, \end{cases} \end{cases} \tag{8}$$

where

$$\mu_{\tilde{g}} = \sum_{i=1}^{N_{\text{VAR}}} \frac{\partial g}{\partial X_i}\bigg|_{\boldsymbol{X}=\boldsymbol{x}^{\text{MPP}}} \frac{\phi(y_i^{\text{MPP}})}{\rho_i(x_i^{\text{MPP}};\boldsymbol{\theta}_i^k)}\left(\eta_i - y_i^{\text{MPP}}\right),$$

$$\sigma_{\tilde{g}} = \sqrt{\sum_{i=1}^{N_{\text{VAR}}} \left(\frac{\partial g}{\partial X_i}\bigg|_{\boldsymbol{X}=\boldsymbol{x}^{\text{MPP}}} \frac{\phi(y_i^{\text{MPP}})}{\rho_i(x_i^{\text{MPP}};\boldsymbol{\theta}_i^k)}\right)^2}. \tag{9}$$

Here, $\beta_t = \Phi^{-1}(P_s)$ is the target reliability index which can be corrected by any SORM approach or Monte Carlo sampling. So far, four SORM approaches have been implemented, e.g. Breitung, Hohenbichler and Tvedt. In addition, Halton- and Hammersley-based importance sampling at the MPP are also implemented. The optimal solution to (8), denoted η_i^*, is mapped back from the standard normal space to the physical space using

$$\mu_i^{k+1} \approx \mu_i^k + \frac{\Phi(Y_i^k)}{\rho_i(\mu_i^k;\boldsymbol{\theta}_i^k)}\eta_i^*.$$

Then, a new QP-problem is generated around $\boldsymbol{\mu}^{k+1}$ and this procedure continues in sequence until convergence is obtained. The QP-problem in (8) solved using `quadprog.m` in Matlab.

3 SUPPORT VECTOR MACHINE

In this section, we present the dual formulation of the soft non-linear support vector machine. First we introduce the original linear SVM, which actually was suggested already in the 60s by Vapnik, then we apply the kernel trick and, finally, regularize the problem.

Let us consider N sampling points $\boldsymbol{x}^i$, which take values $y^i = 1$ (fail) or $y^i = -1$ (safe). Furthermore, we assume that it exists hyper-planes

$$\boldsymbol{w} \cdot \boldsymbol{x} + b = 0, \tag{10}$$

which separate these sampling points into two subsets; one that only takes values $y^i = 1$ and the other one with values $y^i = -1$. This is shown in Figure 1, where the SVM-based RBDO methodology is illustrated. We also assume that the following constraints are satisfied:

$$y^i(\boldsymbol{w}\cdot\boldsymbol{x}^i + b) \geq 1, \quad i = 1,\ldots,N. \tag{11}$$

The shortest distances to $\boldsymbol{x}^i$ from a hyper-plane defined in (10) is given by

$$\boldsymbol{x}^i = \boldsymbol{x} + \gamma^i\frac{\boldsymbol{w}}{\|\boldsymbol{w}\|}. \tag{12}$$

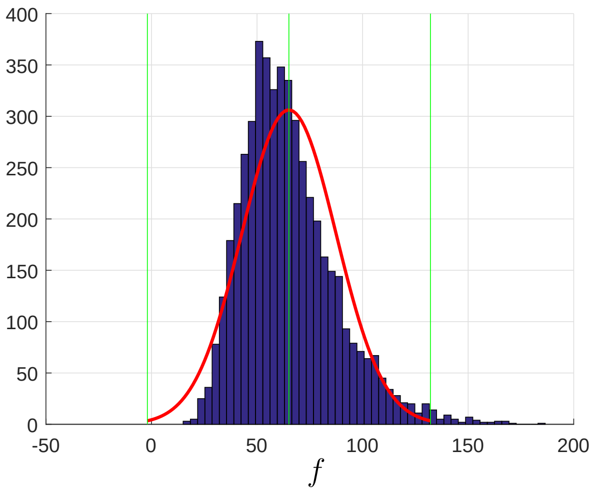

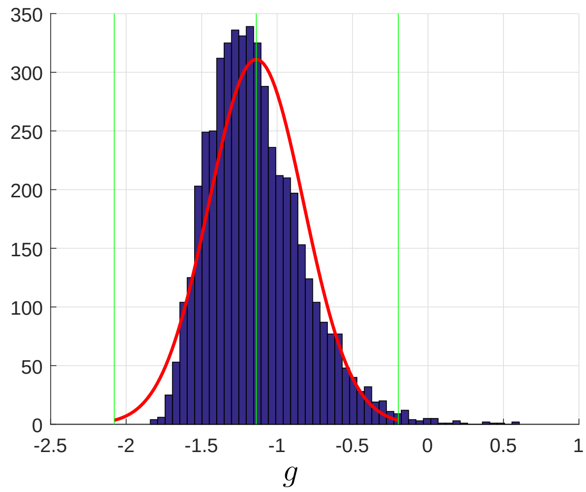

Figure 3: Histogram of the objective function f and the constraint g for the solution obtained by using the SVM. Red lines are showing the corresponding normal distribution, where green lines mark the $\mu \pm 3\sigma$ intervals.

(12) inserted in (11) yields

$$y^i(\boldsymbol{w} \cdot \boldsymbol{x} + b + \gamma^i \|\boldsymbol{w}\|) \geq 1. \tag{13}$$

By utilizing (10), one obtains

$$\gamma^i \geq 1/\|\boldsymbol{w}\| \quad \text{for } y^i = 1, \tag{14a}$$

$$\gamma^i \leq -1/\|\boldsymbol{w}\| \quad \text{for } y^i = -1. \tag{14b}$$

Thus, the lower bound on the shortest distance $|\gamma^i|$ is maximized by minimizing $\|\boldsymbol{w}\|$. This is the key idea of the original linear support vector machine formulation, which reads

$$\begin{cases} \min\limits_{(\boldsymbol{w},b)} \dfrac{1}{2}\|\boldsymbol{w}\|^2 \\ \text{s.t. } 1 - y^i(\boldsymbol{w} \cdot \boldsymbol{x}^i + b) \leq 0, \quad i = 1, \dots N. \end{cases} \tag{15}$$

Obviously, the closest sampling points to the optimal hyper-plane

$$\boldsymbol{w}^* \cdot \boldsymbol{x} + b^* = 0 \tag{16}$$

are obtained when

$$y^i(\boldsymbol{w}^* \cdot \boldsymbol{x}^i + b^*) = 1. \tag{17}$$

Sampling points satisfying (17) are called support vectors, see Figure 1. It is also obvious that in the region between the optimal hyper-plane defined by (16) and the support vectors is empty of sampling points. Thus, the support vector machine formulation in (15) finds a hyper-plane that maximizes the size of this region. This region is augmented with sampling points in the SVM-based adaptive sampling approach discussed in the next section.

The Karush-Kuhn-Tucker conditions of the support vector machine in (15) are given by

$$\boldsymbol{0} = \boldsymbol{w} - \sum_{i=1}^{N} \lambda_i y^i \boldsymbol{x}^i, \tag{18a}$$

$$0 = \sum_{i=1}^{N} \lambda_i y^i, \tag{18b}$$

$$\lambda_i \geq 0, \tag{18c}$$

$$1 - y^i(\boldsymbol{w} \cdot \boldsymbol{x}^i + b) \leq 0, \tag{18d}$$

$$\lambda_i \left(1 - y^i(\boldsymbol{w} \cdot \boldsymbol{x}^i + b)\right) = 0. \tag{18e}$$

The corresponding Lagrangian function is $\mathcal{L} = \mathcal{L}(\boldsymbol{\lambda}, \boldsymbol{w}, b) =$

$$\frac{1}{2}\|\boldsymbol{w}\|^2 + \sum_{i=1}^{N} \lambda_i \left(1 - y^i(\boldsymbol{w} \cdot \boldsymbol{x}^i + b)\right). \tag{19}$$

Furthermore, the dual formulation of the support vector machine in (15) reads

$$\max_{\boldsymbol{\lambda} \geq \boldsymbol{0}} \min_{(\boldsymbol{w},b)} \mathcal{L}(\boldsymbol{\lambda}, \boldsymbol{w}, b). \tag{20}$$

By inserting (18a) in (19), one obtains $\mathcal{L}(\boldsymbol{\lambda}, \boldsymbol{w}(\boldsymbol{\lambda}), b) =$

$$-\frac{1}{2}\sum_{i=1}^{N}\sum_{j=1}^{N} \lambda_i \lambda_j y^i y^j \boldsymbol{x}^i \cdot \boldsymbol{x}^j + \sum_{i=1}^{N} \lambda_i - b\sum_{i=1}^{N} \lambda_i y^i. \tag{21}$$

In addition, the latter part is zero by (18b). In conclusion, the dual support vector machine formulation is

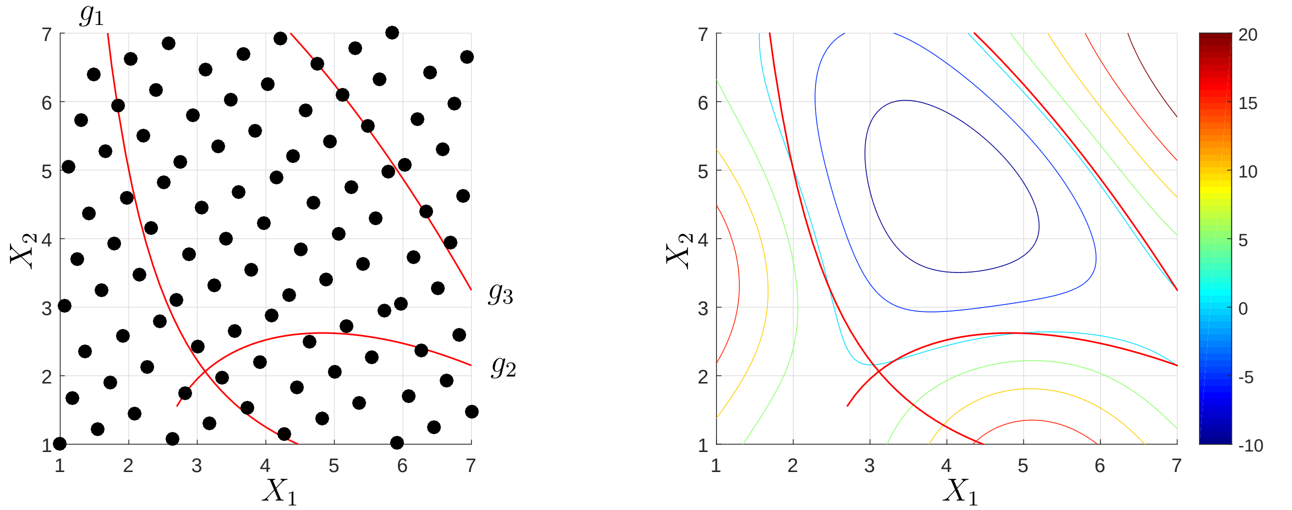

Figure 4: In the left plot the Hammersley sampling of 100 points is shown together with the explicit constraints g_i. To the right the corresponding SVM is depicted. The limit state surface in cyan corresponds well to the actual limit surfaces g_i.

given by

$$\begin{cases} \min_{\boldsymbol{\lambda}} \frac{1}{2} \sum_{i=1}^{N} \sum_{j=1}^{N} \lambda_i \lambda_j y^i y^j \boldsymbol{x}^i \cdot \boldsymbol{x}^j - \sum_{i=1}^{N} \lambda_i \\ \text{s.t.} \begin{cases} \sum_{i=1}^{N} \lambda_i y^i = 0, \\ \lambda_i \geq 0, \quad i = 1, \ldots, N. \end{cases} \end{cases} \tag{22}$$

From the optimal solution $\boldsymbol{\lambda}^*$ of the dual support vector machine in (22), we obtain the corresponding support vector machine solution from the Karush-Kuhn-Tucker conditions in (18) as

$$\boldsymbol{w}^* = \sum_{i=1}^{N} \lambda_i^* y^i \boldsymbol{x}^i \tag{23}$$

and

$$b = 1/y^i - \boldsymbol{w}^* \cdot \boldsymbol{x}^i \tag{24}$$

for any $\lambda_i^* > 0$. Notice, by using (23), the optimal hyper-plane in (16) can be written as

$$\sum_{i=1}^{N} \lambda_i^* y^i \boldsymbol{x}^i \cdot \boldsymbol{x} + b^* = 0. \tag{25}$$

Notice also that you only need to do the summation over support vector indices, because otherwise λ^* equals zero by the KKT-conditions. This is utilized in the implementation in order to speed up the evaluation of the SVM.

For non-separable sets of sampling points $\boldsymbol{x}^i$, the support vector machine approach presented above will of course not work. However, one might transform the sample set to a new space where it become separable, let say by $\boldsymbol{\xi} = \boldsymbol{\xi}(\boldsymbol{x})$. In this new space, the only difference in the derivations of the dual support vector machine in (22) and (25) is the appearance of a new scalar product $< \boldsymbol{\xi}^i, \boldsymbol{\xi}^j >$ instead of $\boldsymbol{x}^i \cdot \boldsymbol{x}^j$. Thus, we do not have to know the explicit expression of the transformation $\boldsymbol{\xi} = \boldsymbol{\xi}(\boldsymbol{x})$, but only the expression of the scalar product of the new space. The explicit expression of this scalar product is known to be the kernel function, i.e.

$$k(\boldsymbol{x}^i, \boldsymbol{x}^j) = < \boldsymbol{\xi}^i(\boldsymbol{x}^i), \boldsymbol{\xi}^j(\boldsymbol{x}^j) > . \tag{26}$$

Consequently, by using an appropriate kernel function in (22) instead of $\boldsymbol{x}^i \cdot \boldsymbol{x}^j$, e.g. the Gaussian kernel

$$k = k(\boldsymbol{x}, \boldsymbol{z}) = \exp\left(- \frac{\|\boldsymbol{x} - \boldsymbol{z}\|^2}{2\sigma^2} \right), \tag{27}$$

the sample set can be separated by

$$\sum_{i=1}^{N} \lambda_i^* y^i k(\boldsymbol{x}^i, \boldsymbol{x}) + b^* = 0. \tag{28}$$

Another kernel function is the polynomial kernel, i.e.

$$k = k(\boldsymbol{x}, \boldsymbol{z}) = (1 + \boldsymbol{x} \cdot \boldsymbol{z})^p. \tag{29}$$

Even if we perform a suitable kernel trick, we might have some misclassified points such that (22) does not converge to a solution. This can be treated by applying a regularization of (22). The established soft regularization of (15) is

$$\begin{cases} \min_{(\boldsymbol{w}, b, \boldsymbol{v})} \frac{1}{2} \|\boldsymbol{w}\|^2 + C \sum_{i=1}^{N} v_i \\ \text{s.t.} \begin{cases} 1 - v_i - y^i(\boldsymbol{w} \cdot \boldsymbol{x}^i + b) \leq 0, \quad i = 1, \ldots N, \\ v_i \geq 0, \quad i = 1, \ldots N. \end{cases} \end{cases} \tag{30}$$

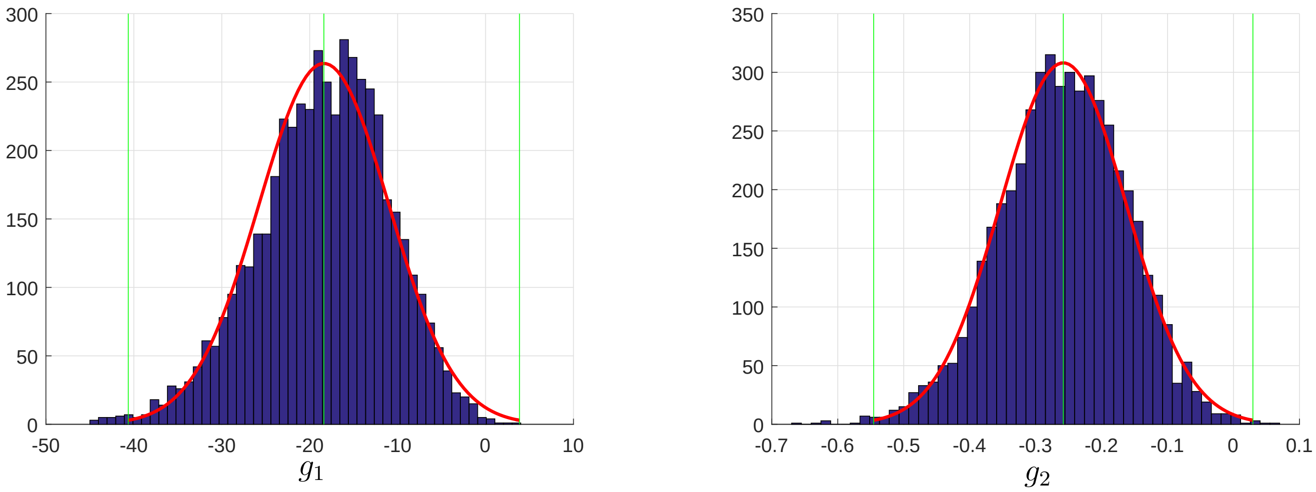

Figure 5: Histograms for the two first active constraints g_1 and g_2, respectively. Red lines are showing the corresponding normal distribution, where green lines mark the $\mu \pm 3\sigma$ intervals.

The Karush-Kuhn-Tucker conditions in (18) then modify by adding the following conditions:

$$C - \lambda_i \geq 0, \tag{31a}$$

$$v_i \geq 0, \tag{31b}$$

$$v_i(C - \lambda_i) = 0. \tag{31c}$$

The corresponding Lagrangian becomes $\mathcal{L} =$

$$-\frac{1}{2}\sum_{i=1}^{N}\sum_{j=1}^{N}\lambda_i\lambda_j y^i y^j \boldsymbol{x}^i \cdot \boldsymbol{x}^j + \sum_{i=1}^{N}\lambda_i - \sum_{i=1}^{N}\lambda_i v_i + C\sum_{i=1}^{N} v_i, \tag{32}$$

where the two latter terms cancel out due to (31c). Thus, the only difference of the dual support vector machine in (22) for this regularization is the appearance of an upper bound on λ_i, i.e.

$$\begin{cases} \min\limits_{\boldsymbol{\lambda}} \dfrac{1}{2}\sum\limits_{i=1}^{N}\sum\limits_{j=1}^{N}\lambda_i\lambda_j y^i y^j k(\boldsymbol{x}^i, \boldsymbol{x}^j) - \sum\limits_{i=1}^{N}\lambda_i \\ \text{s.t.} \begin{cases} \sum\limits_{i=1}^{N}\lambda_i y^i = 0, \\ 0 \leq \lambda_i \leq C, \quad i = 1, \ldots, N. \end{cases} \end{cases} \tag{33}$$

Finally, $0 < \lambda_i < C$ must be satisfied in order for (24) to be valid. Here, we have also introduced the kernel $k(\boldsymbol{x}, \boldsymbol{y})$ in the objective function. The soft non-linear SVM in (33) is solved using `quadprog.m` in Matlab.

4 EXAMPLES

In this section, we demonstrate by solving two examples that the soft non-linear SVM presented in the previous section can represent the limit states properly such that the SQP-based RBDO methodology can be applied for solving RBDO problems with SVM-based limit state functions. The first problem was considered in Strömberg (2016), where SLP-based RBDO was performed by adopting radial basis function networks (RBFN) as metamodels. The second example is a most well-know benchmark for evaluating new RBDO approaches, see e.g. Youn and Choi (2004).

The first example reads

$$\begin{cases} \min\limits_{\mu_i} \sqrt{1000\left(\dfrac{4}{\mu_1} - 2\right)^2 + 1000\left(\dfrac{4}{\mu_1} - 2\right)^2} \\ \text{s.t.} \begin{cases} \Pr[(X_1 - 0.5)^4 + (X_2 - 0.5)^4 \leq 2] \geq P_s, \\ 1 \leq \mu_i \leq 4, \end{cases} \end{cases} \tag{34}$$

where $P_s = 0.999$ and $\mathrm{VAR}[X_i] = 0.1^2$. The deterministic solution is (1.5,1.5) and the minimum of the unconstrained objective function is found at (2,2). The constraint $g > 0$ is plotted to the left in Figure 2. The solution to (34) obtained by our SQP-based RBDO approach is (1.2705,1.2705). The corresponding reliability is 99.9%.

Now, let us consider the problem in (34) as a "black-box", which we represent with metamodels for a sample set of 100 Hammersley points as depicted in Figure 4 for the next example. In particular, we let the objective function be represented by a radial basis function network as in Strömberg (2016) and the limit state is represented by a SVM g^{svm}. In Figure 2, $g^{\text{svm}} > 0$ is plotted. Notice that g^{svm} only represents the limit state properly but not the overall behaviour. Of course, the classification of fail or safe is obtained by taking $\mathrm{sign}(g^{\text{svm}})$. Instead of solving (34), we solve the metamodel-based representation of (34), i.e. the radial basis function taken as our objective function

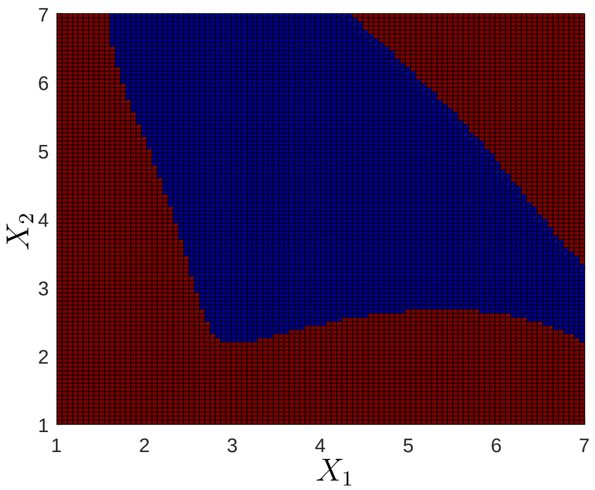

Figure 6: Classification in fail (red) or safe (blue) using the SVM.

and g^{svm} is the limit state function. The corresponding solution is (1.3410, 1.2315) and the reliability for this solution becomes 99.7%, slightly lower than the target of 99.9%. Histograms for the objective function and the constraint are plotted in Figure 3. Notice the non-symmetric characteristic of the solution. This as well as the reliability of the solution can be improved by adopting adaptive sampling. This is a topic for future work. In fact, the SVM is most appropriate for improving the sample set with data along the limit state in the margin of the SVM. Some ideas of how this can be done is outlined for the next example.

The second example is a most well-known benchmark with three constraints and reads

$$
\left\{
\begin{array}{ll}
\min\limits_{\mu_i} & (\mu_1+\mu_2)^2 \\
\text{s.t.} & \left\{
\begin{array}{l}
\Pr[g_1 = 20 - X_1^2 X_2 \le 0] \ge \Phi(3), \\
\Pr\left[\begin{array}{l} g_2 = 1 - \dfrac{(X_1+X_2-5)^2}{30} \\ \quad - \dfrac{(X_1-X_2-12)^2}{120} \le 0 \end{array} \right] \ge \Phi(3), \\
\Pr[g_3 = X_1^2 + 8X_2 - 75 \le 0] \ge \Phi(3), \\
1 \le \mu_i \le 7,
\end{array}
\right.
\end{array}
\right.
\tag{35}
$$

where $\text{VAR}[X_i] = 0.3^2$. A small modification of the original problem is done by taking the square of the objective function. This problem was recently considered in Strömberg (2017) by using a SORM-based SQP approach for reliability based design optimization. The example was in that work also generalized to 50 variables and 75 constraints for five different distributions simultaneously (normal, lognormal, Gumbel, gamma and Weibull). The analytical solution for two variables with normal distribution is obtained to be (3.4525,3.2758) with our RBDO algorithm.

In this work we consider (35) to be a "blackbox" for which we setup a design of experiments using Hammersley sampling with 100 points as shown in Figure 4. From this sampling we define a training set g^{train} for our support vector machine in the following manner:

$$
g^{\text{train}} = \begin{cases} 1 & \text{if any } g_i > 0, \\ -1 & \text{otherwise.} \end{cases} \tag{36}
$$

For this training set, we obtain a SVM g^{svm} according to Figure 4. The plot to the right clearly shows that the the limit state functions are well represented by the global SVM $g^{\text{svm}} = 0$. The corresponding classification of fail or safe using $\text{sign}(g^{\text{svm}})$ is given in Figure 6. As in the previous example, we represent the sampling data for the objective function with a RBFN. Thus, our RBDO problem to be solved is this RBFN-based objective function with the reliability constraint on the SVM $\Pr[g^{\text{svm}} \le 0] \ge \Phi(3)$. In such manner, we reduce the problem size from three constraints to a problem with only one constraint. For this problem, the RBDO algorithm produces the following solution: (3.4247,3.2218). The corresponding reliability indices for the two first active constraints are 2.84 and 2.87, respectively. Histograms for these constraints are given in Figure 5.

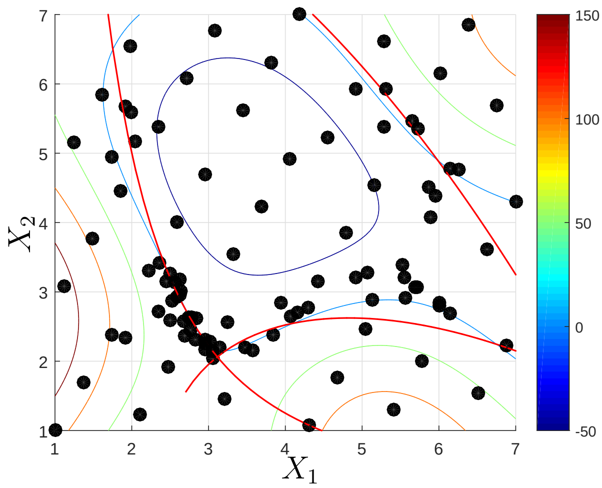

Figure 7: SVM-based adaptive sampling augmented with deterministic optimum and MPP.

Instead of solving (35) using a uniform sampling as presented in Figure 4, we adopt a sequential adaptive sampling approach by distributing points in the margin of the SVM along the limit states as well as adding the deterministic optimum and the most probable point obtained in each sequence. For instance, in Figure 7, we start from a set of 50 Hammersley points and then add 10 points (8 SVM-based points, 1 deterministic optimum, 1 MPP) sequentially five times following this SVM-based sampling approach in order to generate the set of 100 points shown in Figure 7. In this figure the corresponding SVM is also plotted. Comparing the SVMs in Figure 4 and Figure 7, one can see that the latter one better capture the local behavior of the limit surface close to the optimal solution. The optimal solution for this SVM-based formulation of the example is (3.4805,3.2585) and the corresponding reliability indices are 3.08 and 2.95, respectively, for the two active constraints. This is rather close to the target of 3. It is clear that this is an improvement compared to the previous solution presented above for the same example.

Finally, we solve (35) for all three constraints modelled by three separate SVM models using the adaptive DoE used above. Then, we obtain the following solution (3.4304,3.3053), and the corresponding reliability indices for the active constraints: 2.97 and 3.12.

5 CONCLUDING REMARKS

In this work SVM-based RBDO is investigated by implementing soft non-linear SVM together with a SQP-based RBDO method recently developed in Strömberg (2017). The implementation is done so far for two random variables and the idea is to represent the limit state functions with a single SVM. It is demonstrated that the proposed approach works well for an established benchmark with three reliability constraints. It is also demonstrated how the SVM can be utilized in adaptive sampling. For future work it would be interesting to investigate the approach for more than two variables with several constraints.

REFERENCES

Amouzgar, K. & N. Strömberg (2017). Radial basis functions as surrogate models with a priori bias in comparison with a posteriori bias. *Struct. Multidisc. Optim. 55*, 1453–1469.

Basudhar, A., S. Missoum, & A. Sanchez (2008). Limit state function identification using support vector machines for discontinous repsonses and disjoint failure domains. *Probabilistic Engineering Mechanics 23*, 1–11.

Cortes, C. & V. Vapnik (1995). Support-vector networks. *Machine Learning 20*, 273–297.

Hamel, L. (2009). *Knowledge Discovery with Support Vector Machines*. Hoboken, New Jersey: Wiley-Blackwell.

Hu, W., K. Choi, & H. Cho (2016). Reliability-based design optimization of wind turbine blades for fatigue life under dynamic wind load uncertainty. *Struct. Multidisc. Optim. 54*, 953–957.

Khatibinia, M., E. Salajegheh, J. Salajegheh, & M. Fadaee (2013). Reliability-based design optimization of reinforced concrete structures including soil-structure iteraction using a discrete gravitational search algorithm and a proposed metamodel. *Engineering Optimization 45*, 1147–1165.

Li, H., A. Zhao, & K. Tee (2016). Structural reliability analysis of multiple limit state functions using multi-input multi-output support vector machine. *Advances in Mechanical Engineering 8*, 1–11.

Liu, X., W. Yizhong, B. Wang, J. Ding, & H. Jie (2017). An adaptive local range sampling method for reliability-based design optimizatio using support vector machine and kriging model. *Struct. Multidisc. Optim. 55*, 2285–2304.

Lv, X., X. Gu, L. He, Z. D., & W. Liu (2015). Reliability design optimization of vehicle front-end structure for pedestrian lower extremity protection under multiple impact cases. *Thin-Walled Structures 94*, 500–511.

Song, H., K. Choi, I. Lee, L. Zhao, & D. Lamb (2012). Sampling-based rbdo using probabilistic sensitivity analysis and virtual support vector machine. In *ASME 2012 International Design Engineering Technical Conferences and Computers and Information in Engineering Conference IDETC/CIE*, Chicago, Illinois, USA.

Strömberg, N. (2016). Reliability based design optimization by using a slp approach and radial basis function networks. In *ASME 2016 International Design Engineering Technical Conferences and Computers and Information in Engineering Conference IDETC/CIE*, Charlotte, North Carolina, USA.

Strömberg, N. (2017). Reliability-based design optimization using sorm and sqp. *Struct. Multidisc. Optim. 56*, 631–645.

Wang, Y., Y. Xiongqing, & D. Xiaoping (2015). Improved reliability-based optimization with support vector machines and its application in aircraft design. *Mathematical Problems in Engineering 2015*, 1–14.

Yang, I.-T. & W. Husada (2017). Improving classification accuracy for single-loop reliability-based design optimization. In *IMECS 2017 the International MultiConference of Engineers and Computer Scientists*, Hong Kong.

Zhu, P., Y. Zhang, & G. Chen (2011). Metamodeling development for reliability-based design optimization of automotive body structure. *Computers in Industry 62*, 729–741.